Adsorption and Dehydration Reaction of Ethanol to Ethylene on Isomorphous B, Al, and Ga Substitution of H-ZSM-5 Zeolite: An Embedded ONIOM Study

Nattida Maeboonruan
Kasetsart University Kamphaeng Saen Campus
Bundet Boekfa (bundet.b@ku.ac.th)
Kasetsart University https://orcid.org/0000-0002-9281-9405
Thana Maihom
Kasetsart University Kamphaeng Saen Campus
Piti Treesukol
Kasetsart University Kamphaeng Saen Campus
Kanokwan Kongpatpanich
VISTEC: Vidyasirimedhi Institute of Science and Technology
Supawadee Namuangruk
National Nanotechnology Center
Michael Probst
Universität Innsbruck: Universitat Innsbruck
Jumras Limtrakul
VISTEC: Vidyasirimedhi Institute of Science and Technology

Research Article

Keywords: Ethanol, Ethylene, Dehydration, Isomorphously zeolite, Embedded ONIOM

Posted Date: June 7th, 2021

DOI: https://doi.org/10.21203/rs.3.rs-545104/v1

Abstract

Dehydration reactions are important in the petroleum and petrochemical industries, especially for the feedstock production. In this work, the catalytic activity of zeolites with different acidities for the dehydration of ethanol to ethylene was investigated by calculations on cluster models of three isomorphous B, Al, and Ga substitution of H-ZSM-5 zeolites. Detailed reaction profiles for the dehydration reaction, assuming either a stepwise or a concerted mechanism, were calculated by using the ONIOM(MP2:M06-2X) + SCREEP method. The adsorption energies of ethanol are -21.6, -28.1 and -27.7 kcal/mol on H-[B]-ZSM-5, H-[Al]-ZSM-5, H-[Ga]-ZSM-5 zeolites, respectively. The stepwise mechanism was preferred on all isomorphous zeolites. The activation energies for the ethoxy formation as the rate-determining step are in range of 40.0 to 42.3 kcal/mol. The results indicated that the order of catalytic activity were H-[Al]-ZSM-5 > H-[Ga]-ZSM-5 > H-[B]-ZSM-5 for catalyzing the dehydration of ethanol to ethylene. Besides the acid strength, the zeolite framework affected the reaction by stabilizing the reaction intermediates leading to more stable adsorption complexes and lower activation barriers.

Introduction

Zeolites are used as catalysts in the petrochemical industries due to their remarkable properties such as selectivity control, thermal stability, and tunable acid strength.[1–4] Among a large number of reactions catalyzed by zeolites, dehydration reactions are especially important. Dehydration is widely accepted as the key reaction involved in the conversion of biomass into value-added chemicals. For example, bioethanol from fermentation processes can be changed to ethylene, an important feedstock for polymer production.[5–8] Several zeolites have been reported to use for an environmentally friendly biomass conversion.[3, 9] Several techniques such as nuclear magnetic resonance (NMR) and Infrared (IR) spectroscopy are commonly used to observe the reaction species.[10–12] There were several experimental studies on the dehydration of ethanol to ethylene with H-[Al]-ZSM-5 zeolite.[13–15] The dehydration reaction of ethanol were also studied over Sn-Beta zeolite [16], Ni-ZSM-5 [17]. The ethoxy group was considered to be an intermediate for the dehydration of ethanol to ethylene. [18, 19] The details of adsorption and reaction of the dehydration of ethanol on acidic zeolite have been previously studied by several computational methods. The ethanol dehydration over H-ZSM-5, H-BEA and H-AEL were studied with ONIOM calculation.[20]The ONIOM (DFT:UFF) method was used to study the adsorption of ethanol, 1-propanol, and 1-butanol on H-ZSM-5 zeolite.[21] The comparison of the adsorption heats of ethanol on H-ZSM-5 zeolite and on silicalite revealed the confinement effect of the framework on the adsorption properties.[22] Several density functional theory (DFT) studied on the dehydration reaction of ethanol have been performed to determine the reaction mechanism and the effects of acid strength and zeolite framework on it. [18, 23–27] Recently, more evidence was reported from experimental study as the oxonium ion was observed during the ethanol dehydration reaction. [28]

Zeolites isomorphously substituted with several metals have been examined to obtain guideline for designing new enhanced catalysts. Isomorphous substitutions of B, Fe, Ga and Al into the ZSM-5 zeolite framework were studied by Fourier transform infrared spectroscopy and temperature-programmed

ammonia desorption techniques.[29] The relative Brønsted acidity (OH) order of modified zeolites was found to be Si < B < < Fe < Ga < Al. Density functional calculations were used to determine the acid strength of the substituted zeolites.[30–33] Deka *et al.* studied the effect of substitutions with Al, B and Ga by using a cluster model and suggested that the acidity trend of the catalysts can be derived from their relative electrophilicities.[31] The order of the acidities of isomorphously metal substituted ZSM-5 determined from adsorption of ammonia, was B < Fe < Ga < Al, which was in agreement with experimental result.[32] The same acidity trend was found for larger pore size H-MCM-22.[34, 35] The aromatization of furans by dehydration on Al, Fe, Ga and B in BEA zeolite was studied by a combination of calculations and experiment.[36] The H-[B]-BEA zeolite was determined to be the weakest acid with H-[Al]-BEA being the strongest one. Recently, catalytic properties of Ga-modified hierarchical H-ZSM-5 nanosheets for the aromatization of C5 hydrocarbons was also demonstrated.[37]

The confinement effect was suggested to be crucial for the interaction between the zeolite framework and adsorbed molecules since confinement can alter physisorption and activation energies.[38] These effects on unsaturated aliphatic, aromatic and heterocyclic compounds were theoretically examined by a combination of second order Møller-Plesset perturbation theory (MP2) and hybrid density functional M06-2X.[39] The M06 functionals[40] developed by the Truhlar group had also been successfully used for studying adsorption and reactions on acidic Zeolites[39, 41, 42], on Lewis-acid zeolites[43, 44], on metallic catalysts[45–49], and on organic molecules[50, 51]. Recently they have been applied to determine P-NMR chemical shifts of phosphorus-modified CHA zeolite.[52] These higher adsorption energy and lower activation barrier caused by the confinement effect, determined from hybrid functional DFT calculation, were in good agreement with experimental results.[39, 53] While reaction mechanisms of the dehydration of the ethanol to ethylene on several zeolite catalysts have been investigated,[23, 36] no systematic investigation of zeolites with various acid strengths catalyzing the dehydration of ethanol has been reported.

In this work, the ethanol adsorption and its dehydration reaction on isomorphously metal (B, Al or Ga) substituted H-ZSM-5 were investigated by means of the ONIOM method. ONIOM is a methodology that allows to combine highly accurate calculations of reaction centers with lower accuracy calculations of the environment. [54] The inner layer 5T cluster containing the Brønsted acid was treated with the highly accurate MP2 method while the framework 34T cluster represented the zeolite framework was treated with the M06-2X DFT. All atoms of the first two layers were embedded into point charges to represent the zeolitic Madelung potential from an infinite lattice generated by the SCREEP method.[39] The objective of this study was to determine the effect of the acidity of the substituted zeolite on the adsorption and dehydration reaction.

Methodology

The adsorption and dehydration reaction of ethanol on H-ZSM-5 zeolites have been theoretically studied with a combination of MP2 and DFT calculations. Brønsted acid strengths of isomorphously metal-substituted ZSM-5 zeolites are calculated and discussed. The 34T (T: tetrahedra of Si, B, Al and Ga

atoms) quantum clusters, as shown in Figure S1 in the supporting information, were tailored from the crystallographic coordinates to represent the active region and the nearby zigzag channel of zeolite. The metal modified zeolites were prepared by substituting the silicon atom at T12 position of ZSM-5 cluster with either B, Al or Ga atoms, denoted as H-[B]-ZSM-5, H-[Al]-ZSM-5 and H-[Ga]-ZSM-5 zeolites, respectively. The ONIOM[54] scheme was applied on the 34T clusters to represent both the active Brønsted acid site and the confinement effect as well as the extended framework in a feasible way.[55] Geometry optimization was performed using the ONIOM(MP2:M06-2X) model. The inner 5T quantum cluster covering the Brønsted acid and all adsorbed species was optimized at the MP2 level and the outer 34T quantum cluster was treated with the DFT/M06-2X functional. To reduce computational cost, only the inner 5T layer and the adsorbed species were relaxed while the outer 34T layer were kept fixed at its crystallographic position. The 6-31G(d,p) basis set was used for structure optimization. Then, single point calculations with the 6-311 + G(2df,2p) basis set were performed on top of these. Several adsorption modes of ethanol on the zeolite surface were studied.

The consequence of the long-range electrostatic potential from the infinite zeolite lattice, represented by embedded point charges[56, 57], has often been stressed. The long range effects represented by the embedded-ONIOM (e-ONIOM) method was found to be crucial for the adsorption and reaction on zeolites.[39, 58, 59] The 5T:34T model of H-[Al]-ZSM-5 with embedded ONIOM(MP2/6-311 + G(2df,2p):M06-2X/6-311 + G(2df,2p)) on the optimized structure at ONIOM(MP2/6-31G(d,p):M06-2X/6-31G(d,p))) level of theory is shown in Fig. 1. Two possible mechanisms proposed for the ethanol dehydration reaction are shown in scheme 1. The transition states were determined by the Berny algorithm and were confirmed by a single negative- normal mode corresponding to their reaction pathway. All calculations were performed with the Gaussian 09 program[60].

Results And Discussion

The optimized structural parameters of all H-ZSM-5 zeolite determined from ONIOM(MP2:M06-2X) hierarchical model with embedded point charge are shown in Table S1 in the supporting information. This AlŸŸŸHz distance was similar to experimental data (2.40 Å).[61] The Brønsed acid O1-Hz distances were 0.97 Å for all metal-substituted zeolites. The BŸŸŸHz, AlŸŸŸHz and GaŸŸŸHz distances were 2.34, 2.36 and 2.42 Å, respectively. The average B-O_{avg}, Al-O_{avg} and Ga-O_{avg} bond distances are 1.54, 1.72 and 1.79 Å while the experimental B-O_{avg} bond and Ga-O_{avg} bond were 1.59 and 1.60 Å, respectively.[62] The Mulliken charges of Hz of Brønsted acid were + 0.30, + 0.34 and + 0.35 |e|, respectively while the charges of substituted metal atoms were + 1.08, + 0.38 and + 0.62 |e| for B, Al and Ga, respectively. The partial charge of the Al atom in the zeolite framework was significantly less positive than those of B and Ga atoms and could possibly affect the adsorption and the reaction path.

The optimized structures of the ethanol adsorption on H-[Al]-ZSM-5 are illustrated in Fig. 2. Their structural parameters are tabulated in tables S3 in the supporting information. For H-[Al]-ZSM-5 three adsorption modes have been found: bound by one hydrogen bond (side on, AD-Al-1A), doubly hydrogen

bond (end on at zigzag channel, AD-Al-1B), and protonated (end on at the intersection, AD-Al-1C) as shown in Fig. 2.

For the single and doubly hydrogen-bond adsorption complexes, the intermolecular O-Hz distances were 1.42 Å for AD-Al-1A and 1.36 Å for AD-Al-1B. The protonated O-Hz distance in AD-Al-1C was 1.00 Å. The protonated ethanol-adsorption on zeolite was previously reported in a periodic model study.[24] The ethanol-zeolite interaction causes electron transfer from the ethanol to the Brønsted site of zeolite. The changes of the partial charge of ethanol upon the adsorption were + 0.04, + 0.13 and + 0.04 |e|, for AD-Al-1A, AD-Al-1B and AD-Al-1C, respectively. The adsorption energies are − 23.3, -29.8 and − 28.1 kcal/mol, respectively. These value agreed with the experimental value of -31.0 kcal/mol for ethanol on H-[Al]-ZSM-5.[22] The effect of the zeolite framework on the adsorption energies was further investigated. The extended framework of zeolite contributes to 25–27 % of the adsorption energy. The energy details are given in table S6 of the supporting information.

Three modes of ethanol adsorption on H-[B]-ZSM-5 and H-[Ga]-ZSM-5 were examined as well (Figures S2 and S4 and Tables S2 and S4 of the supporting information). All three types of adsorption were found for the high acid strength H-[Ga]-ZSM-5 zeolite: singly hydrogen bond (side on, AD-Ga-1A), doubly hydrogen bond (end on at zigzag channel, AD-Ga-1B) and protonation form (end on at intersection region, AD-Ga-1C). On the other hand, only the H-bond types were found for the lower acid strength H-[B]-ZSM-5 zeolite: singly (side on, AD-B-1A), and doubly hydrogen bond (end on at zigzag channel, AD-B-1B). The adsorption energies are − 23.2, -29.4 and − 27.7 kcal/mol for AD-Ga-1A, AD-Ga-1B and AD-Ga-1C, respectively, and − 19.0, -23.1 and − 21.6 kcal/mol for AD-B-1A, AD-B-1B and AD-B-1C, respectively. The partial charge donated to ethanol is + 0.05, + 0.17 and + 0.27 |e| for AD-Ga-1A, AD-Ga-1B and AD-Ga-1C, respectively, and 0.00, + 0.06 and + 0.03 |e| for AD-B-1A, AD-B-1B and AD-B-1C, respectively. The lower amount of charge transfer from H-[B]-ZSM-5 to ethanol coincide with the lower adsorption energy. The charge transfer for H-[Ga]-ZSM-5 is comparable with the one in H-[Al]-ZSM-5. Altogether, the trend of the adsorption energies is the same as found previously for the adsorption of ammonia: H-[B]-ZSM-5 < H-[Ga]-ZSM-5 < H-[Al]-ZSM-5.[30, 34]

The differences in adsorption energy of small molecule calculated at high level can be used to differentiate the acid strength of the Brønsted acid site. The adsorption energies of ethanol on the 5T Brønsted acid site of zeolite at the high level of ONIOM were − 16.7 kcal/mol on AD-B-1B, -22.2 kcal/mol on AD-Al-1B and − 21.6 kcal/mol on AD-Ga-1B, respectively. Inclusion of the framework increased these adsorption energies by -6.4, -7.6 and − 7.8 kcal/mol for AD-B-1B, AD-Al-1B and AD-Ga-1B, respectively. The adsorption energies decrease in the order H-[Al]-ZSM-5 > H-[Ga]-ZSM-5 > H-[B]-ZSM-5 and the contribution of the extended framework effect to the adsorption energy was 23–27 %. The strongest absorption occurred on H-[Al]-ZSM-5. All adsorption energies are tabulated in table S5-7 of the supporting information.

The adsorption of the ethylene was examined in the same way. The structures of the adsorption complexes are shown in Figure S5 of the supporting information. The π-bond of ethylene interacted with

the hydrogen atom of zeolite. The intermolecular C -Hz distances were 2.16 for H-[Al]-ZSM-5 and 2.20 Å for H-[Ga]-ZSM-5 while on H-[B]-ZSM-5 they are slightly longer. The adsorption energies of ethylene were − 11.6, -14.7 and − 14.5 kcal/mol for H-[B]-ZSM-5, H-[Al]-ZSM-5 and H-[Ga]-ZSM-5, respectively. These energies were comparable to an experimentally derived adsorption energy of ethylene on H-FAU of -9 kcal/mol.[63] The framework contributed more in the adsorption of the ethylene than that of the ethanol. It increased the adsorption energy by 34% for H-[B]-ZSM-5, by 31% for H-[Al]-ZSM-5 and by 29% for H-[Ga]-ZSM-5 as shown in table S9 of the supporting information.

Two reaction pathways for the dehydration reaction on H-[Al]-ZSM-5, a stepwise and a concerted mechanism, are shown in Scheme 1. The stepwise mechanism proceeded via an ethoxide intermediate. The adsorption, intermediate, product and transition state structures are shown in Figure S8 and selected geometrical parameters are tabulated in Table S14 in the supporting information. The energy profiles of both mechanisms were given in Fig. 3. The reaction started with the protonated form of the AD-Al-1C complex where the adsorption energy of ethanol was − 28.1 kcal/mol. The ethoxide intermediate was formed on the oxygen of zeolite and then a water molecule was produced. The transition state (TS1-Al) had one imaginary frequency at 1113.9i cm^{-1} corresponding to the breaking of the C1-O bond and the formation of the C1-O2 bond. This step was the rate determining with a relative activation energy of 11.9 kcal/mol and the total activation energy of 35.2 kcal/mol. It was compared with the value of 28.2 kcal/mol from a periodic calculation [24], with 44.6–49.1 kcal/mol from a simpler ONIOM scheme (5T ONIOM(M06-2X:PM6) [23] and with the 25.1 kcal/mol [18] for the bare 3T cluster.

The formation of the ethoxide intermediate was endothermic relative to the adsorption complex. Its C-O bond length of 1.53 Å was typical for a covalent bond. The energies calculated from different levels of calculations are tabulated in Table S15. The framework effect decreased the activation energy from 43.4 to be 40.0 kcal/mol and stabilized the ethoxide intermediate by -7.5 kcal/mol. The desorption energy of the water molecule produced from the alkoxide intermediate [IN2-Al] was 5.3 kcal/mol, comparable with an experimental desorption energy of water inside silicate of 7.17 kcal/mol.[22] The framework of zeolite had a larger role in this desorption energy than in the active site. Finally, the relative energy of the alkoxide intermediate [IN2-Al] was − 2.2 kcal/mol before transforming to ethylene.

For the ethylene formation, the second transition state (TS2-Al) led to C1-O bond cleavage and the hydrogen transfer to the oxygen of zeolite. The relative activation energy was 28.5 kcal/mol with one imaginary frequency at 417.3i cm^{-1}. The relative energy of the ethylene product (PR-Al) was 0.7 kcal/mol with a desorption energy of 14.7 kcal/mol.

The other possible mechanism was the concerted one as shown in Fig. 4. The optimized structures for the concerted pathway are shown in Figure S9 and Table S16 in the supporting information. The adsorption AD-Al-1A was observed to correspond the concerted reaction pathway. The transition state (TSc-Al) with one imaginary frequency at 852.3i cm^{-1} led to the breaking of the O-H bond of zeolite and the C-H bond of ethanol. The products from this step were ethylene and water (PRc-Al) with a relative energy of 42.6 kcal/mol. A previous study with ONIOM(M062X:PM6) level of calculation reported the

adsorption energies in the range of 43.1–48.1 kcal/mol.[23] The lower activation barrier of TS1-Al compared to TSc-Al indicated that the concerted mechanism was thermodynamically inferior to the stepwise one even though the differences in the relative energies of the transition state were not large.

The framework effects are illustrated in table S15 and S17 of the supporting information. The high-level calculation (5T) represented the effect from Brønsted acid energy and provided the activation barrier of 40.0, 30.7 and 42.6 kcal/mol for the TS1-Al, TS2-Al and TSc-Al, respectively. The apparent activation barriers are 11.9, 28.5 and 19.3 kcal/mol, respectively. For H-[Al]-ZSM-5, the effect of the framework reduced the total activation energy by 7–12% for TS1-Al and TS2-Al of the stepwise mechanism. However, the framework had no significantly influence on TSc-Al of the concerted mechanism.

The effect of acid strength on the reaction mechanisms was studied by comparing H-[B]-ZSM-5 and H-[Ga]-ZSM-5. The respective reaction profiles are given in Figs. 5 and 6 and the reaction mechanisms on H-[B]-ZSM-5 and H-[Ga]-ZSM-5 zeolites in Figs. 7 and 8. The adsorption energies followed the trend H-[Al]-ZSM-5 ~ H-[Ga]-ZSM-5 > H-[B]-ZSM-5. The optimized structures and their energies for the stepwise and concerted pathway are shown in Figures S6-S7 and Table S10-S13 on H-[B]-ZSM-5 and Figures S10-S11 and table S18-S21 on H-[B]-ZSM-5 of the supporting information. For a lower acid strength zeolite H-[B]-ZSM-5, the total activation energies were 42.3, 38.9 and 48.5 kcal/mol for TS1-B, TS2-B and TSc-B, respectively. The alkoxide formation transition state was stabilized by the framework by about 7%. The boron alkoxide intermediate IN1-B was more stable than IN1-Al and IN1-Ga. The C-O bond distance of 1.48 Å indicated the strong covalent bond. Due to the stabilized alkoxide intermediate, the activation barrier of the second step at TS2-B was higher than the ones at TS2-Al and TS2-Ga.

For the reaction on the H-[Ga]-ZSM-5, the total activation energies were 41.1, 29.1 and 43.6 kcal/mol for TS1-Ga, TS2-Ga and TSc-Ga, respectively. The framework decreased the activation energy by 8–13% for the stepwise and by only 3% for the concerted mechanisms. This showed that H-[Al]-ZSM-5 and H-[Ga]-ZSM-5 were the competitive catalysts for the dehydration reaction. Our results agreed very well with the previous experimental studies reporting that the dehydration of ethanol was more selective to ethylene on H-[Ga]-ZSM-5 with 94.6 %yield, while the %yield to ethylene on H-[Al]-ZSM-5 was only 40.6.[64] The energies of the first transition states of TS1-Al and TS1-Ga were nearly the same. However, the second transition state of H-[Ga]-ZSM-5 was slightly lower than that of H-[Al]-ZSM-5. Then, in case of H-[Al]-ZSM-5 the oligomerization to propene via a diethyl ether was another competitive reaction pathway. [13] Finally, the thermal free energies were calculated with the ONIOM (MP2:M06-2X) method and shown in energy profile in Figs. 9 and 10. The activation energies for the reaction on H-[Ga]-ZSM-5 were not different to be 40.1 and 43.1 kcal/mol for the TS1-Ga and TSc-Ga, respectively. The activation barrier trends were H-[Al]-ZSM-5 > H-[Ga]-ZSM-5 > H-[B]-ZSM-5.

Table 1
Reaction energies for the stepwise mechanism of the ethanol reduction on the 5T:34T cluster models of the three H-ZSM-5 zeolites as calculated with the embedded ONIOM(MP2:M06-2X) method. [a]

	AD-1C	TS1	IN1	IN2	TS2	PR
H-[B]-ZSM-5						
Embedded ONIOM [b]	-21.6	**20.7** (42.3)	-11.8	-2.8	**36.1** (38.9)	3.8
MP2 [c]	-15.8	**30.0** (45.8)	-2.1	-1.0	**38.7** (39.7)	7.7
H-[Al]-ZSM-5						
Embedded ONIOM [b]	-28.1	**11.9** (40.0)	-7.5	-2.2	**28.5** (30.7)	0.7
MP2 [c]	-18.9	**24.5** (43.4)	0.0	-1.4	**33.6** (35.0)	5.1
H-[Ga]-ZSM-5						
Embedded ONIOM [b]	-27.7	**13.4** (41.1)	-6.0	0.4	**29.5** (29.1)	0.9
MP2 [c]	-20.2	**24.8** (45.0)	1.8	0.8	**34.3** (33.5)	5.1

[a] Apparent activation energies are presented in bold type, while intrinsic activation energies are in parentheses. Energies are given in kcal/mol

[b] ONIOM(MP2/6-311 + G(2df,2p):M06-2X/6-311 + G(2df,2p))//ONIOM(MP2/6-31G(d,p):M06-2X/6-31G(d,p) model 5T:34T

[c] MP2/6-311 + G(2df,2p)//ONIOM(MP2/6-31G(d,p):M06-2X/6-31G(d,p) model 5T

Table 2
Reaction energies for the concerted mechanism of the ethanol reduction on the 5T:34T cluster models of the three H-ZSM-5 zeolites as calculated with the embedded ONIOM(MP2:M06-2X) method. [a]

	AD-1A	TSc	INc	PRc
H-[B]-ZSM-5				
Embedded ONIOM [b]	-19.0	**29.5** (48.5)	-4.4	4.9
MP2 [c]	-14.9	**33.5** (48.4)	6.7	11.8
H-[Al]-ZSM-5				
Embedded ONIOM [b]	-23.3	**19.3** (42.6)	-4.4	5.1
MP2 [c]	-17.1	**25.3** (42.4)	4.3	11.2
H-[Ga]-ZSM-5				
Embedded ONIOM [b]	-23.2	**20.4** (43.6)	-2.0	7.4
MP2 [c]	-16.8	**25.3** (42.1)	5.6	11.7

[a] Apparent activation energies are presented in bold type, while intrinsic activation energies are in parentheses. Energies are in kcal/mol

[b] ONIOM(MP2/6-311 + G(2df,2p):M06-2X/6-311 + G(2df,2p))//ONIOM(MP2/6-31G(d,p):M06-2X/6-31G(d,p) model 5T:34T

[c] MP2/6-311 + G(2df,2p)//ONIOM(MP2/6-31G(d,p):M06-2X/6-31G(d,p) model 5T

Conclusions

The dehydration of ethanol on three H-[M]-ZSM-5 zeolites which were obtained by isomorphous substitution of a Si atom at the T12 position of the original structure with either a B, Al or Ga atom have been studied within the ONIOM(MP2:M06-2X) + SCREEP method. A protonation interaction at the channel-intersection of ZSM-5 was only found on the H-[Al]-ZSM-5 and H-[Ga]-ZSM-5 zeolites. The adsorption strengths of ethanol were in the order H-[Al]-ZSM-5 > H-[Ga]-ZSM-5 > H-[B]-ZSM-5 with the adsorption energies of -28.1, -27.7 and -21.6 kcal/mol, respectively. Stepwise and concerted reaction

pathways have been proposed as possible reaction mechanisms. Activation energies for the stepwise mechanism were 40.0 and 30.7 kcal/mol for H-[Al]-ZSM-5, 41.1 and 29.1 kcal/mol for H-[Ga]-ZSM-5, and 42.3 and 38.9 kcal/mol for H-[B]-ZSM-5, respectively. The first step involving the alkoxide formation has been found to be the rate-determining step. Its activation energies for the concerted mechanisms were 42.6, 43.6 and 48.5 for H-[Al]-ZSM-5 > H-[Ga]-ZSM-5 > H-[B]-ZSM-5, slightly larger than those of the stepwise mechanisms. The geometrical and electronic effects of the extended framework amounted to 23-27 % of the adsorption energy and 7-12% of the energy of the transition state. The results indicated that the order of catalytic activity will be H-[Al]-ZSM-5 > H-[Ga]-ZSM-5 > H-[B]-ZSM-5. Therefore, the first two zeolites are suitable for the dehydration reaction of ethanol.

Declarations

Acknowledgements:

Nattida Maeboonruan acknowledges a Science Technology, Engineering, Mathematics (STEM) grant SCA-CO-2561-6176-TH. Bundet Boekfa acknowledges the Thailand Research Fund (TRF) grant MRG6080103; Kasetsart Research and Development Institute (KURDI) and the Faculty of Liberal Arts and Science Kasetsart University. The supported from the Thailand Graduate Institute of Science and Technology (TGIST); the National e-Science Infrastructure consortium; the Graduate School Kasetsart University; the Ministry of Higher Education, Science, Research and Innovation; the Thai Agro Energy Public Company Limited are also acknowledged.

Funding: This work was supported by Science Technology, Engineering, Mathematics (STEM) grant SCA-CO-2561-6176-TH and the Thailand Research Fund (TRF) grant MRG6080103.

Conflicts of interest/Competing interests: The authors declare no conflicts of interest.

Availability of data and material: N/A

Code availability: N/A

Authors' contributions:
Nattida Maeboonruan: Investigation, Methodology and Writing
Bundet Boekfa: Supervision, Conceptualization, Investigation, Methodology and Writing.
Thana Maihom: Conceptualization and Investigation.
Piti Treesukol: Conceptualization and Writing.
Kanokwan Kongpatpanich: Conceptualization and Investigation.
Supawadee Namuangruk: Conceptualization and Investigation.
Michael Probst: Conceptualization and Writing.
Jumras Limtrakul: Conceptualization and Investigation.

References

[1] A. Corma (2003) State of the art and future challenges of zeolites as catalysts. J. Catal. 216: 298-312 https://doi.org/10.1016/S0021-9517(02)00132-X

[2] B. Smit, T.L.M. Maesen (2008) Towards a molecular understanding of shape selectivity. Nature 451: 671-678 https://doi.org/10.1038/nature06552

[3] A. Corma , S. Iborra, A. Velty (2007) Chemical routes for the transformation of biomass into chemicals. Chem. Rev. 107: 2411-2502 https://doi.org/10.1021/cr050989d

[4] A. Bhan, E. Iglesia (2008) A link between reactivity and local structure in acid catalysis on zeolites. Acc. Chem. Res. 41: 559-567 https://doi.org/10.1021/ar700181t

[5] D. Fan, D.J. Dai, H.S. Wu (2013) Ethylene formation by catalytic dehydration of ethanol with industrial considerations. Materials 6: 101-115 https://doi.org/10.3390/ma6010101

[6] A. Morschbacker (2009) Bio-ethanol based ethylene. Polymer Reviews 49: 79-84 https://doi.org/10.1080/15583720902834791

[7] I. Takahara, M. Saito, M. Inaba, K. Murata (2005) Dehydration of ethanol into ethylene over solid acid catalysts. Catal. Lett. 105: 249-252 https://doi.org/10.1007/s10562-005-8698-1

[8] V.F. Tret'yakov, Y.I. Makarfi, K.V. Tret'yakov, N.A. Frantsuzova, R.M. Talyshinskii (2010) The catalytic conversion of bioethanol to hydrocarbon fuel: A review and study. Catalysis in Industry 2: 402-420 https://doi.org/10.1134/S2070050410040161

[9] A.J.J. Straathof (2014) Transformation of biomass into commodity chemicals using enzymes or cells. Chem.Rev. 114: 1871-1908 https://doi.org/10.1021/cr400309c

[10] J.F. Haw, T. Xu (1998) NMR Studies of Solid Acidity. Advances in Catalysis 42: 115-180 https://doi.org/10.1016/S0360-0564(08)60628-8

[11] C. Lamberti, E. Groppo, G. Spoto, S. Bordiga, A. Zecchina (2007) Infrared Spectroscopy of Transient Surface Species. Advances in Catalysis 51: 1-74 https://doi.org/10.1016/S0360-0564(06)51001-6

[12] W. Wang, M. Seiler, M. Hunger (2001) Role of surface methoxy species in the conversion of methanol to dimethyl ether on acidic zeolites investigated by in situ stopped-flow MAS NMR spectroscopy. J. Phys. Chem. B 105: 12553-12558 https://doi.org/10.1021/jp0129784

[13] R. Batchu, V.V. Galvita, K. Alexopoulos, T.S. Glazneva, H. Poelman, M.F. Reyniers, G.B. Marin (2020) Ethanol dehydration pathways in H-ZSM-5: Insights from temporal analysis of products. Catal. Today 355: 822-831 https://doi.org/10.1016/j.cattod.2019.04.018

[14] Z. Wang, L.A. O'Dell, X. Zeng, C. Liu, S. Zhao, W. Zhang, M. Gaborieau, Y. Jiang, J. Huang (2019) Insight into Three-Coordinate Aluminum Species on Ethanol-to-Olefin Conversion over ZSM-5 Zeolites.

Angewandte Chemie - International Edition 58: 18061-18068 https://doi.org/10.1002/anie.201910987

[15] C.Y. Wu, H.S. Wu (2017) Ethylene Formation from Ethanol Dehydration Using ZSM-5 Catalyst. ACS Omega 2: 4287-4296 https://doi.org/10.1021/acsomega.7b00680

[16] B.C. Bukowski, J.S. Bates, R. Gounder, J. Greeley (2018) First principles, microkinetic, and experimental analysis of Lewis acid site speciation during ethanol dehydration on Sn-Beta zeolites. J. Catal. 365: 261-276 https://doi.org/10.1016/j.jcat.2018.07.012

[17] D.T. Sarve, S.K. Singh, J.D. Ekhe (2020) Kinetic and mechanistic study of ethanol dehydration to diethyl ether over Ni-ZSM-5 in a closed batch reactor. Reaction Kinetics, Mechanisms and Catalysis 131: 261-281 https://doi.org/10.1007/s11144-020-01847-z

[18] J.N. Kondo, D. Nishioka, H. Yamazaki, J. Kubota, K. Domen, T. Tatsumi (2010) Activation energies for the reaction of ethoxy species to ethene over zeolites. Journal of Physical Chemistry C 114: 20107-20113 https://doi.org/10.1021/jp107082t

[19] J.N. Kondo, K. Ito, E. Yoda, F. Wakabayashi, K. Domen (2005) An ethoxy intermediate in ethanol dehydration on Brønsted acid sites in zeolite. J. Phys. Chem. B 109: 10969-10972 https://doi.org/10.1021/jp050721q

[20] L.Y. Kunz, L. Bu, B.C. Knott, C. Liu, M.R. Nimlos, R.S. Assary, L.A. Curtiss, D.J. Robichaud, S. Kim (2019) Theoretical determination of size effects in zeolite-catalyzed alcohol dehydration. Catalysts 9: 700 https://doi.org/10.3390/catal9090700

[21] R.J. Costa, E.A.S. Castro, J.R.S. Politi, R. Gargano, J.B.L. Martins (2019) Methanol, ethanol, propanol, and butanol adsorption on H-ZSM-5 zeolite: an ONIOM study. J. Mol. Model. 25: 34 https://doi.org/10.1007/s00894-018-3894-2

[22] C.C. Lee, R.J. Gorte, W.E. Farneth (1997) Calorimetric study of alcohol and nitrile adsorption complexes in H-ZSM-5. J. Phys. Chem. B 101: 3811-3817 https://doi.org/10.1021/jp970711s

[23] S. Kim, D.J. Robichaud, G.T. Beckham, R.S. Paton, M.R. Nimlos (2015) Ethanol dehydration in HZSM-5 studied by density functional theory: Evidence for a concerted process. J. Phys. Chem. A 119: 3604-3614 https://doi.org/10.1021/jp513024z

[24] K. Alexopoulos, M. John, K. Van Der Borght, V. Galvita, M.F. Reyniers, G.B. Marin (2016) DFT-based microkinetic modeling of ethanol dehydration in H-ZSM-5. J. Catal. 339: 173-185 https://doi.org/10.1016/j.jcat.2016.04.020

[25] C.M. Nguyen, M.F. Reyniers, G.B. Marin (2010) Theoretical study of the adsorption of C1-C4 primary alcohols in H-ZSM-5. Physical Chemistry Chemical Physics 12: 9481-9493 https://doi.org/10.1039/c000503g

[26] C.M. Nguyen, M.F. Reyniers, G.B. Marin (2015) Adsorption thermodynamics of C1-C4 alcohols in H-FAU, H-MOR, H-ZSM-5, and H-ZSM-22. J. Catal. 322: 91-103 https://doi.org/10.1016/j.jcat.2014.11.013

[27] K. Alexopoulos, M.S. Lee, Y. Liu, Y. Zhi, Y. Liu, M.F. Reyniers, G.B. Marin, V.A. Glezakou, R. Rousseau, J.A. Lercher (2016) Anharmonicity and Confinement in Zeolites: Structure, Spectroscopy, and Adsorption Free Energy of Ethanol in H-ZSM-5. Journal of Physical Chemistry C 120: 7172-7182 https://doi.org/10.1021/acs.jpcc.6b00923

[28] X. Zhou, C. Wang, Y. Chu, J. Xu, Q. Wang, G. Qi, X. Zhao, N. Feng, F. Deng (2019) Observation of an oxonium ion intermediate in ethanol dehydration to ethene on zeolite. Nature Communications 10: 1961 https://doi.org/10.1038/s41467-019-09956-7

[29] C.T.W. Chu, C.D. Chang (1985) Isomorphous substitution in zeolite frameworks. 1. Acidity of surface hydroxyls in [B]-, [Fe]-, [Ga]-, and [Al]-ZSM-5. J. Phys. Chem. 89: 1569-1571 https://doi.org/10.1021/j100255a005

[30] S. Jungsuttiwong, J. Lomratsiri, J. Limtrakul (2011) Characterization of acidity in [B], [Al], and [Ga] isomorphously substituted ZSM-5: Embedded DFT/UFF approach. Int. J. Quantum Chem. 111: 2275-2282 https://doi.org/10.1002/qua.22531

[31] R.C. Deka, R. Vetrivel, S. Pal (1999) Application of Hard-Soft Acid-Base Principle to Study Brönsted Acid Sites in Zeolite Clusters: A Quantum Chemical Study. J. Phys. Chem. A 103: 5978-5982 https://doi.org/10.1021/jp984267k

[32] S.P. Yuan, J.G. Wang, Y.W. Li, H. Jiao (2002) Brønsted acidity of isomorphously substituted ZSM-5 by B, Al, Ga, and Fe. Density functional investigations. J. Phys. Chem. A 106: 8167-8172 https://doi.org/10.1021/jp025792t

[33] S.P. Yuan, J.G. Wang, Y.W. Li, H. Jiao (2004) Density functional investigations into the siting of Fe and the acidic properties of isomorphously substituted mordenite by B, Al, Ga and Fe. Journal of Molecular Structure: THEOCHEM 674: 267-274 https://doi.org/10.1016/S0166-1280(03)00463-9

[34] Y. Wang, G. Yang, D. Zhou, X. Bao (2004) Density functional theory study of chemical composition influence on the acidity of H-MCM-22 zeolite. J. Phys. Chem. B 108: 18228-18233 https://doi.org/10.1021/jp049384w

[35] Y. Wang, D. Zhou, G. Yang, S. Miao, X. Liu, X. Bao (2004) A DFT study on isomorphously substituted MCM-22 zeolite. J. Phys. Chem. A 108: 6730-6734 https://doi.org/10.1021/jp0376875

[36] R.E. Patet, M. Koehle, R.F. Lobo, S. Caratzoulas, D.G. Vlachos (2017) General Acid-Type Catalysis in the Dehydrative Aromatization of Furans to Aromatics in H-[Al]-BEA, H-[Fe]-BEA, H-[Ga]-BEA, and H-[B]-BEA Zeolites. Journal of Physical Chemistry C 121: 13666-13679 https://doi.org/10.1021/acs.jpcc.7b02344

[37] W. Wannapakdee, D. Suttipat, P. Dugkhuntod, T. Yutthalekha, A. Thivasasith, P. Kidkhunthod, S. Nokbin, S. Pengpanich, J. Limtrakul, C. Wattanakit (2019) Aromatization of C5 hydrocarbons over Ga-modified hierarchical HZSM-5 nanosheets. Fuel 236: 1243-1253 https://doi.org/10.1016/j.fuel.2018.09.093

[38] E.G. Derouane, C.D. Chang (2000) Confinement effects in the adsorption of simple bases by zeolites. Microporous Mesoporous Mater. 35-36: 425-433 https://doi.org/https://doi.org/10.1016/S1387-1811(99)00239-5

[39] B. Boekfa, S. Choomwattana, P. Khongpracha, J. Limtrakul (2009) Effects of the zeolite framework on the adsorptions and hydrogen-exchange reactions of unsaturated aliphatic, aromatic, and heterocyclic compounds in ZSM-5 zeolite: A combination of perturbation theory (MP2) and a newly developed density functional theory (M06-2X) in ONIOM scheme. Langmuir 25: 12990-12999 https://doi.org/10.1021/la901841w

[40] Y. Zhao, D.G. Truhlar (2008) The M06 suite of density functionals for main group thermochemistry, thermochemical kinetics, noncovalent interactions, excited states, and transition elements: Two new functionals and systematic testing of four M06-class functionals and 12 other functionals. Theor. Chem. Acc. 120: 215-241 https://doi.org/10.1007/s00214-007-0310-x

[41] B. Boekfa, P. Pantu, M. Probst, J. Limtrakul (2010) Adsorption and tautomerization reaction of acetone on acidic zeolites: The confinement effect in different types of zeolites. Journal of Physical Chemistry C 114: 15061-15067 https://doi.org/10.1021/jp1058947

[42] S. Klinyod, B. Boekfa, S. Pornsatitworakul, T. Maihom, N. Jarussophon, P. Treesukol, C. Wattanakit, J. Limtrakul (2019) Theoretical and Experimental Study on the 7-Hydroxy-4-Methylcoumarin Synthesis with H-Beta Zeolite. ChemistrySelect 4: 10660-10667 https://doi.org/10.1002/slct.201902596

[43] Y. Injongkol, T. Maihom, S. Choomwattana, B. Boekfa, J. Limtrakul (2017) A mechanistic study of ethanol transformation into ethene and acetaldehyde on an oxygenated Au-exchanged ZSM-5 zeolite. RSC Advances 7: 38052-38058 https://doi.org/10.1039/c7ra06313j

[44] V. Paluka, T. Maihom, C. Warakulwit, P. Srifa, B. Boekfa, P. Treesukol, P. Poolmee, J. Limtrakul (2020) Density functional study of the effect of cation exchanged Sn-Beta zeolite for the diels-alder reaction between furan and methyl acrylate. Chem. Phys. Lett. 754: 137743 https://doi.org/https://doi.org/10.1016/j.cplett.2020.137743

[45] B. Boekfa, E. Pahl, N. Gaston, H. Sakurai, J. Limtrakul, M. Ehara (2014) C-Cl bond activation on Au/Pd bimetallic nanocatalysts studied by density functional theory and genetic algorithm calculations. Journal of Physical Chemistry C 118: 22188-22196 https://doi.org/10.1021/jp5074472

[46] B. Boekfa, P. Treesukol, Y. Injongkol, T. Maihom, P. Maitarad, J. Limtrakul (2018) The activation of methane on Ru, Rh, and Pd decorated carbon nanotube and boron nitride nanotube: A DFT study.

Catalysts 8: 190. https://doi.org/10.3390/catal8050190

[47] S. Ketrat, T. Maihom, P. Treesukul, B. Boekfa, J. Limtrakul (2019) Theoretical study of methane adsorption and C—H bond activation over Fe-embedded graphene: Effect of external electric field. J. Comput. Chem. 40: 2819-2826 https://doi.org/10.1002/jcc.26058

[48] N. Pueyo Bellafont, G. Álvarez Saiz, F. Viñes, F. Illas (2016) Performance of Minnesota functionals on predicting core-level binding energies of molecules containing main-group elements. Theor. Chem. Acc. 135: 1-9 https://doi.org/10.1007/s00214-015-1787-3

[49] A. Gupta, B. Boekfa, H. Sakurai, M. Ehara, U.D. Priyakumar (2016) Structure, Interaction, and Dynamics of Au/Pd Bimetallic Nanoalloys Dispersed in Aqueous Ethylpyrrolidone, a Monomeric Moiety of Polyvinylpyrrolidone. J. Phys. Chem. C 120: 17454-17464 https://doi.org/10.1021/acs.jpcc.6b05097

[50] P. Nimnual, J. Tummatorn, B. Boekfa, C. Thongsornkleeb, S. Ruchirawat, P. Piyachat, K. Punjajom (2019) Construction of 5-Aminotetrazoles via in Situ Generation of Carbodiimidium Ions from Ketones Promoted by $TMSN_3$/TfOH. J. Org. Chem. 84: 5603-5613 https://doi.org/10.1021/acs.joc.9b00555

[51] K. Khownium, J. Romsaiyud, S. Borwornpinyo, P. Wongkrasant, P. Pongkorpsakol, C. Muanprasat, B. Boekfa, T. Vilaivan, S. Ruchirawat, J. Limtrakul (2019) Turn-on fluorescent sensor for the detection of lipopolysaccharides based on a novel bispyrenyl terephtalaldehyde-bis-guanylhydrazone. New J. Chem. 43: 7051-7056 https://doi.org/10.1039/c9nj00323a

[52] P. Zhao, B. Boekfa, T. Nishitoba, N. Tsunoji, T. Sano, T. Yokoi, M. Ogura, M. Ehara (2020) Theoretical study on 31P NMR chemical shifts of phosphorus-modified CHA zeolites. Microporous Mesoporous Mater. 294: 109908 https://doi.org/10.1016/j.micromeso.2019.109908

[53] K. Kongpatpanich, T. Nanok, B. Boekfa, M. Probst, J. Limtrakul (2011) Structures and reaction mechanisms of glycerol dehydration over H-ZSM-5 zeolite: A density functional theory study. Physical Chemistry Chemical Physics 13: 6462-6470 https://doi.org/10.1039/c0cp01720e

[54] S. Dapprich, I. Komáromi, K.S. Byun, K. Morokuma, M.J. Frisch (1999) A new ONIOM implementation in Gaussian98. Part I. The calculation of energies, gradients, vibrational frequencies and electric field derivatives. Journal of Molecular Structure: THEOCHEM 461-462: 1-21 https://doi.org/10.1016/S0166-1280(98)00475-8

[55] E.G. Derouane (1998) Zeolites as solid solvents. J. Mol. Catal. A: Chem. 134: 29-45 https://doi.org/10.1016/S1381-1169(98)00021-1

[56] E.V. Stefanovich, T.N. Truong (1996) Embedded density functional approach for calculations of adsorption on ionic crystals. J. Chem. Phys. 104: 2946-2955 https://doi.org/10.1063/1.471115

[57] M. Allavena, K. Seiti, E. Kassab, G. Ferenczy, J.G. Ángyán (1990) Quantum-chemical model calculations on the acidic site of zeolites including Madelung-potential effects. Chem. Phys. Lett. 168: 461-467 https://doi.org/10.1016/0009-2614(90)85144-2

[58] T. Maihom, B. Boekfa, J. Sirijaraensre, T. Nanok, M. Probst, J. Limtrakul (2009) Reaction mechanisms of the methylation of ethene with methanol and dimethyl ether over h-zsm-5: An ONIOM study. Journal of Physical Chemistry C 113: 6654-6662 https://doi.org/10.1021/jp809746a

[59] B. Boekfa, P. Pantu, J. Limtrakul (2008) Interactions of amino acids with H-ZSM-5 zeolite: An embedded ONIOM study. J. Mol. Struct. 889: 81-88 https://doi.org/10.1016/j.molstruc.2008.01.026

[60] M.J. Frisch, ; Trucks, G. W.; Schlegel, H. B.; Scuseria, G. E.; Robb, M. A.; Cheeseman, J. R.; Scalmani, G.; Barone, V.; Mennucci, B.; Petersson, G. A.; Nakatsuji, H.; Caricato, M.; Li, X.; Hratchian, H. P.; Izmaylov, A. F.; Bloino, J.; Zheng, G.; Sonnen Trucks, G. W.; Schlegel, H. B.; Scuseria, G. E.; Robb, M. A.; Cheeseman, J. R.; Scalmani, G.; Barone, V.; Mennucci, B.; Petersson, G. A.; Nakatsuji, H.; Caricato, M.; Li, X.; Hratchian, H. P.; Izmaylov, A. F.; Bloino, J.; Zheng, G.; Sonnenberg, J. L.; Hada, M.; Ehara, M.; Toyota, K.; Fukuda, R.; Hasegawa, J.; Ishida, M.; Nakajima, T.; Honda, Y.; Kitao, O.; Nakai, H.; Vreven, T.; Montgomery, J. A., Jr.; Peralta, J. E.; Ogliaro, F.; Bearpark, M.; Heyd, J. J.; Brothers, E.; Kudin, K. N.; Staroverov, V. N.; Kobayashi, R.; Normand, J.; Raghavachari, K.; Rendell, A.; Burant, J. C.; Iyengar, S. S.; Tomasi, J.; Cossi, M.; Rega, N.; Millam, N. J.; Klene, M.; Knox, J. E.; Cross, J. B.; Bakken, V.; Adamo, C.; Jaramillo, J.; Gomperts, R.; Stratmann, R. E.; Yazyev, O.; Austin, A. J.; Cammi, R.; Pomelli, C.; Ochterski, J. W.; Martin, R. L.; Morokuma, K.; Zakrzewski, V. G.; Voth, G. A.; Salvador, P.; Dannenberg, J. J.; Dapprich, S.; Daniels, A. D.; Farkas, Ö.; Foresman, J. B.; Ortiz, J. V.; Cioslowski, J.; Fox, D. J. (2009) Gaussian 09, Gaussian, Inc., Wallingford CT.:

[61] D. Freude, J. Klinowski, H. Hamdan (1988) Solid-state NMR studies of the geometry of brønsted acid sites in zeolitic catalysts. Chem. Phys. Lett. 149: 355 - 362 https://doi.org/10.1016/0009-2614(88)85107-8

[62] L. Palin, C. Lamberti, Å. Kvick, F. Testa, R. Aiello, M. Milanesio, D. Viterbo (2003) Single-crystal synchrotron radiation X-ray diffraction study of B and Ga silicalites compared to a purely siliceous MFI: A discussion of the heteroatom distribution. J. Phys. Chem. B 107: 4034-4042 https://doi.org/10.1021/jp027586r

[63] N.W. Cant, W.K. Hall (1972) Studies of the hydrogen held by solids. XXI. The interaction between ethylene and hydroxyl groups of a Y-zeolite at elevated temperatures. J. Catal. 25: 161-172 https://doi.org/10.1016/0021-9517(72)90213-8

[64] Y. Furumoto, Y. Harada, N. Tsunoji, A. Takahashi, T. Fujitani, Y. Ide, M. Sadakane, T. Sano (2011) Effect of acidity of ZSM-5 zeolite on conversion of ethanol to propylene. Applied Catalysis A: General 399: 262-267 https://doi.org/10.1016/j.apcata.2011.04.009

Figures

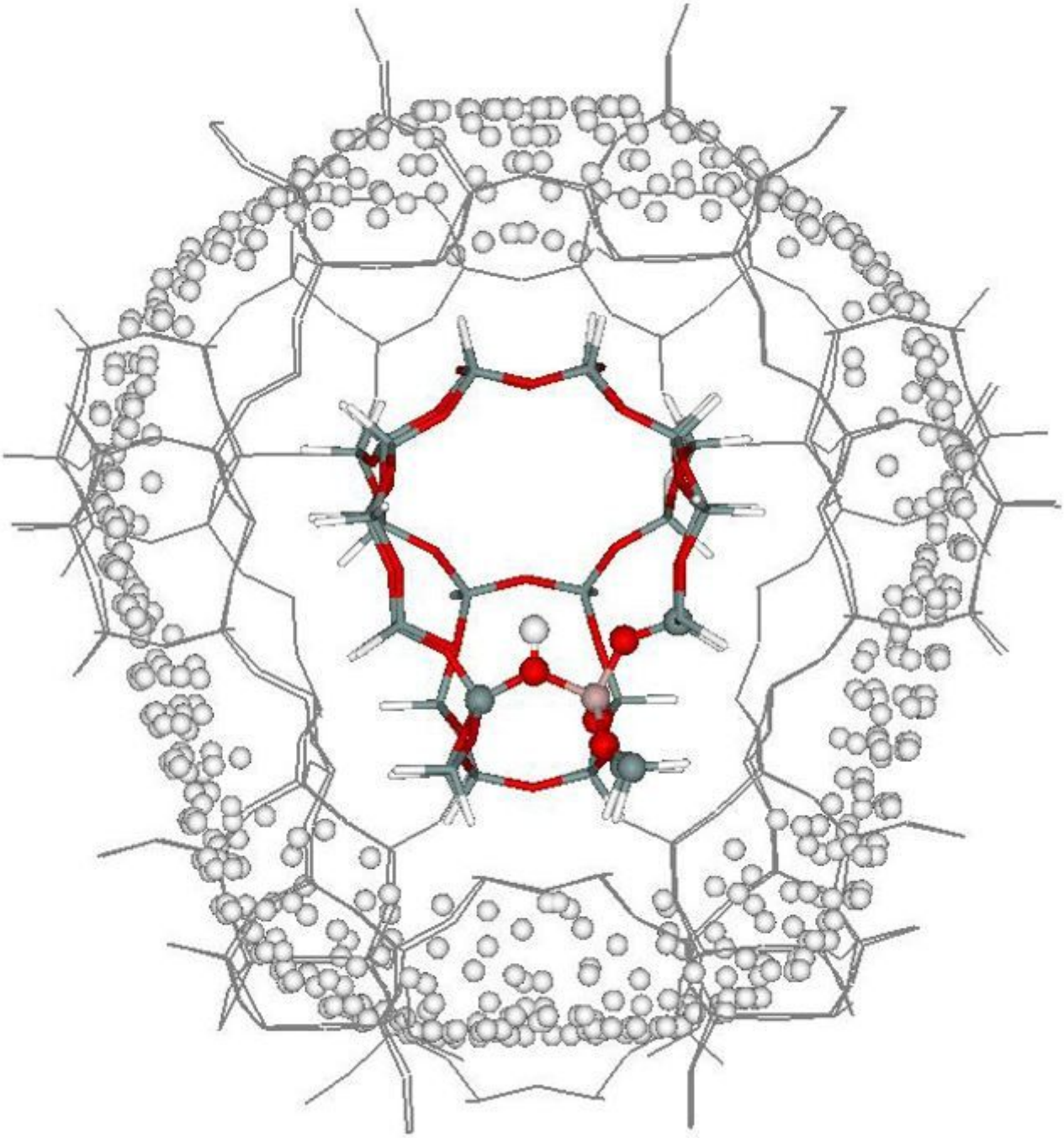

Figure 1

Structure of H-[Al]-ZSM-5 zeolite model 5T:34T with the embedded ONIOM (MP2/6-311+G(2df,2p):M06-2X/6-311+G(2df,2p)) // ONIOM (MP2/6-31G(d,p):M06-2X/6-31G(d,p)) as described in the text. Atoms treated at the MP2 level of theory are shown as balls (Red color is oxygen, Pink color is Aluminum, Gray color is Silicon and White color is hydrogen). Lines are bonds between atoms for which the M06-2X functional is used. The embedded point charges surrounding the cluster are shown as white balls and thin line frame.

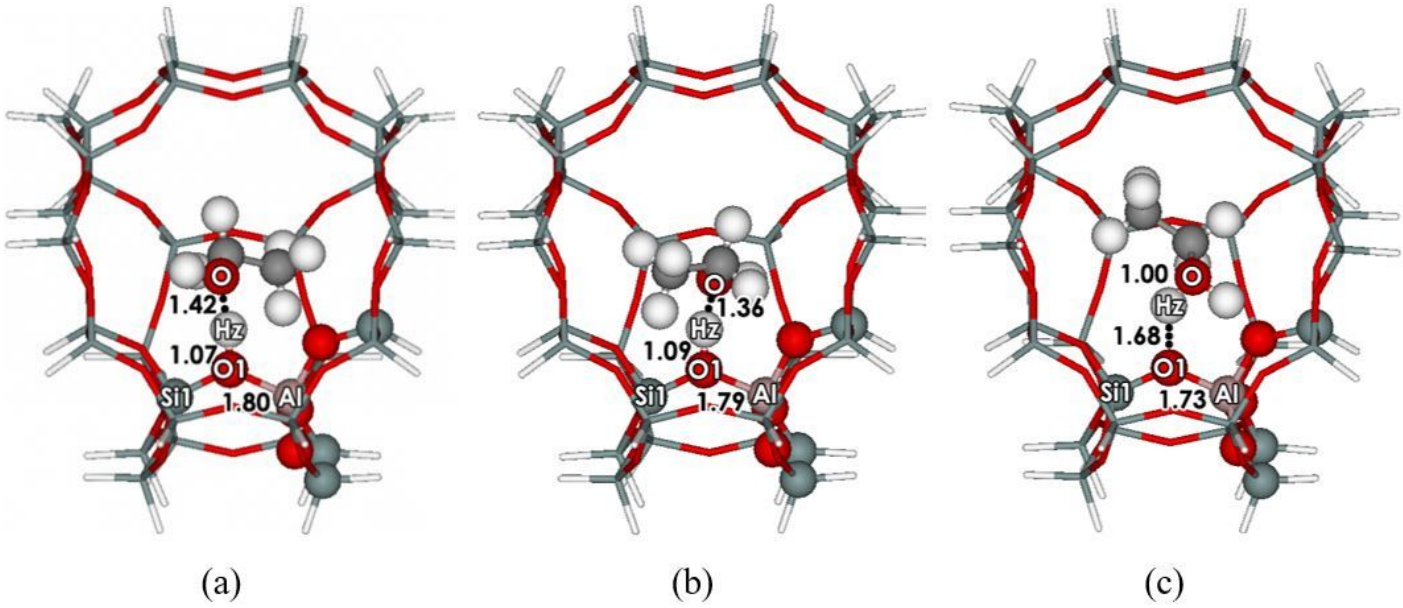

Figure 2

Optimized structures of ethanol adsorptions as calculated on the 5T:34T model of H-[Al]-ZSM-5 with the ONIOM (MP2/6-31G(d,p):M06-2X/6-31G(d,p)) method: (a) one hydrogen bond (side on, AD-Al-1A), (b) double hydrogen bond (end on at zigzag channel, AD-Al-1B) and (c) protonation (end on at intersection region, AD-Al-1C). Distances are given in Å.

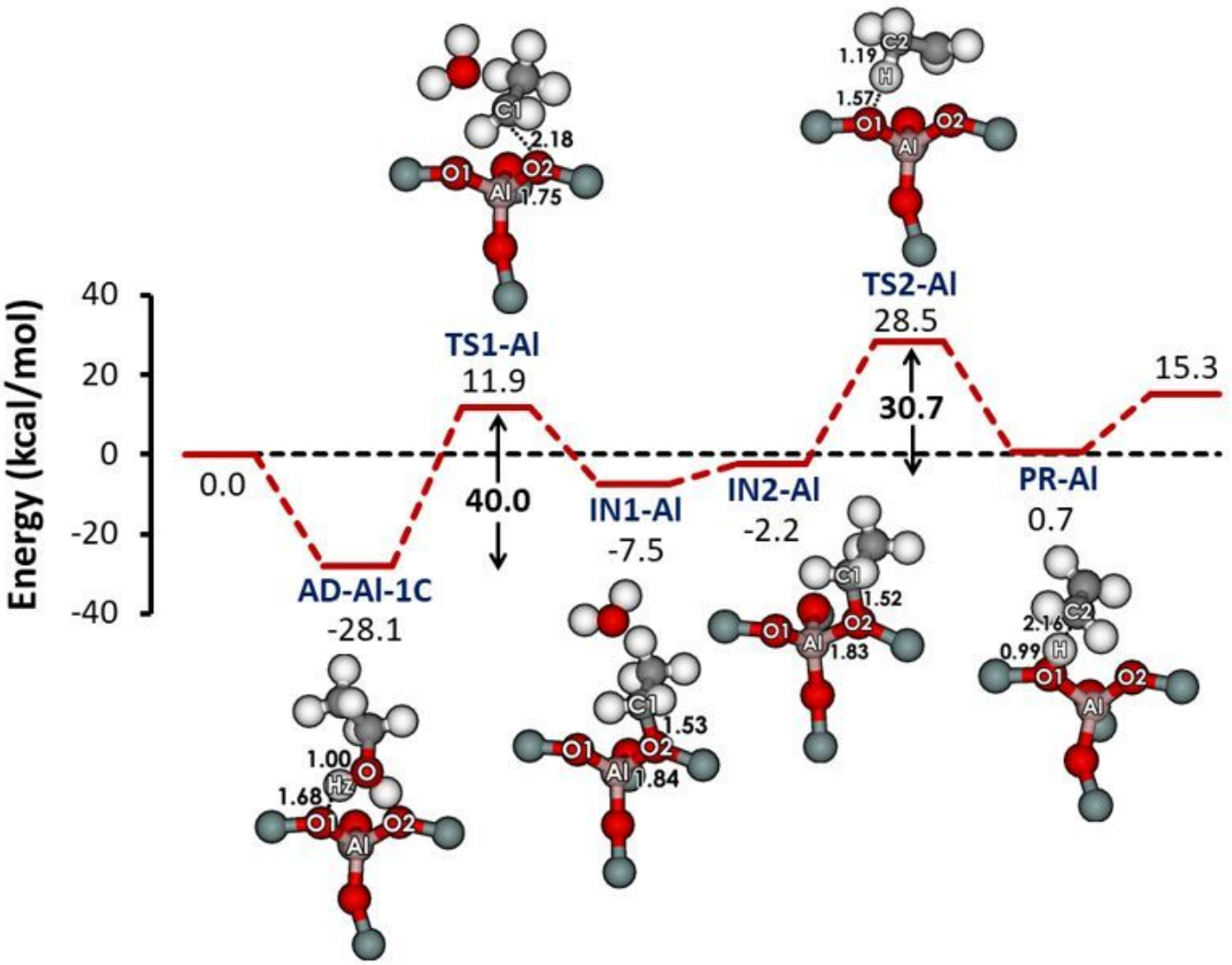

Figure 3

Energy profile for the stepwise reaction of ethanol to ethylene on 5T:34T model of H-[Al]-ZSM-5 zeolites as calculated with the embedded ONIOM (MP2/6-311+G(2df,2p):M06-2X/6-311+G(2df,2p)) // ONIOM (MP2/6-31G(d,p):M06-2X/6-31G(d,p)). Distances are given in Å and energies in kcal/mol.

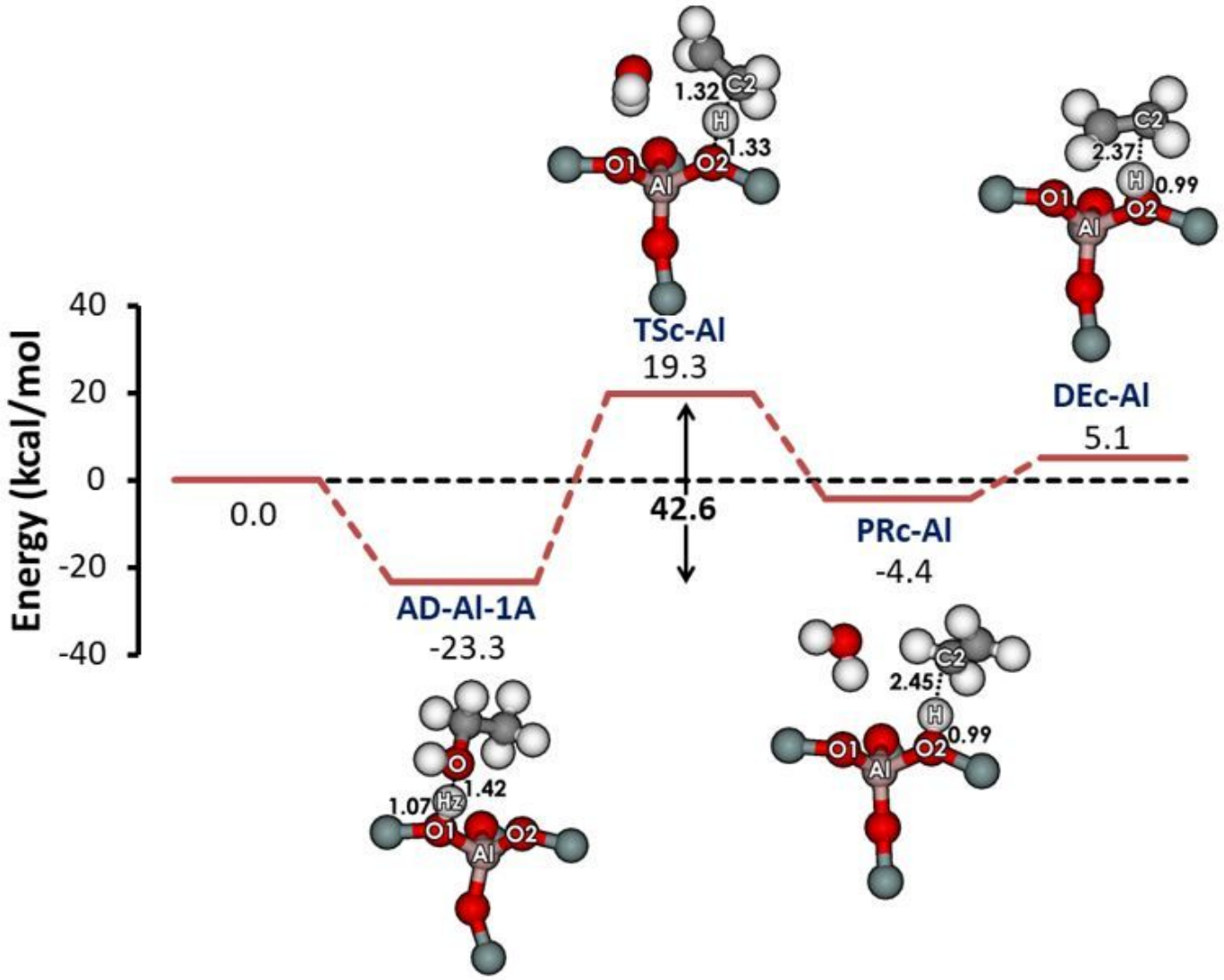

Figure 4

Energy profile for the concerted reaction of ethanol to ethylene on 5T:34T model of H-[Al]-ZSM-5 zeolites as calculated with the embedded ONIOM (MP2/6-311+G(2df,2p):M06-2X/6-311+G(2df,2p)) // ONIOM (MP2/6-31G(d,p):M06-2X/6-31G(d,p)). Distances are given in Å and energies in kcal/mol.

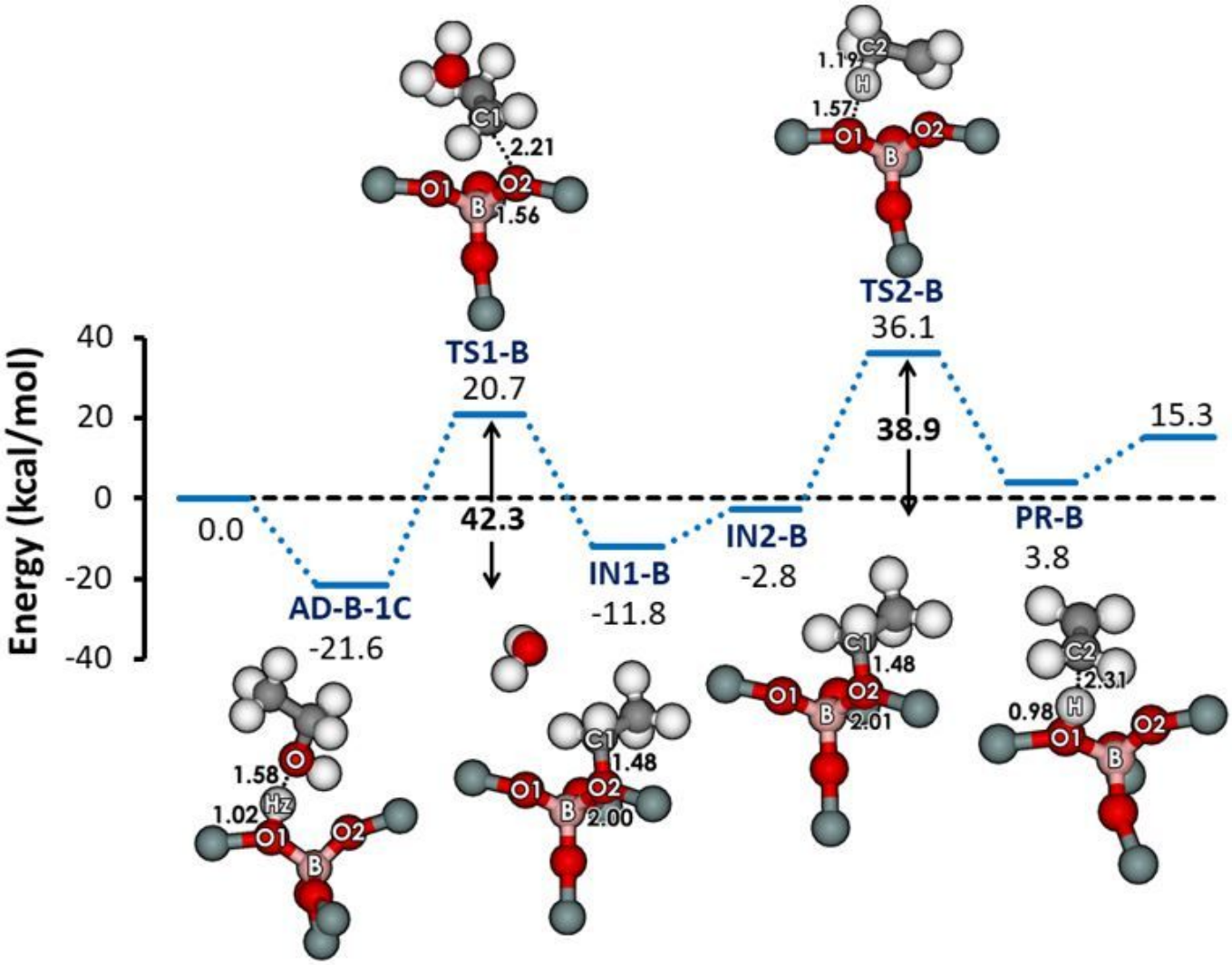

Figure 5

Energy profile for the stepwise mechanism on the 5T:34T model of H-[B]-ZSM-5 zeolite with the embedded ONIOM (MP2/6-311+G(2df,2p):M06-2X/6-311+G(2df,2p)) // ONIOM (MP2/6-31G(d,p):M06-2X/6-31G(d,p)). Distances are given in Å and energies in kcal/mol.

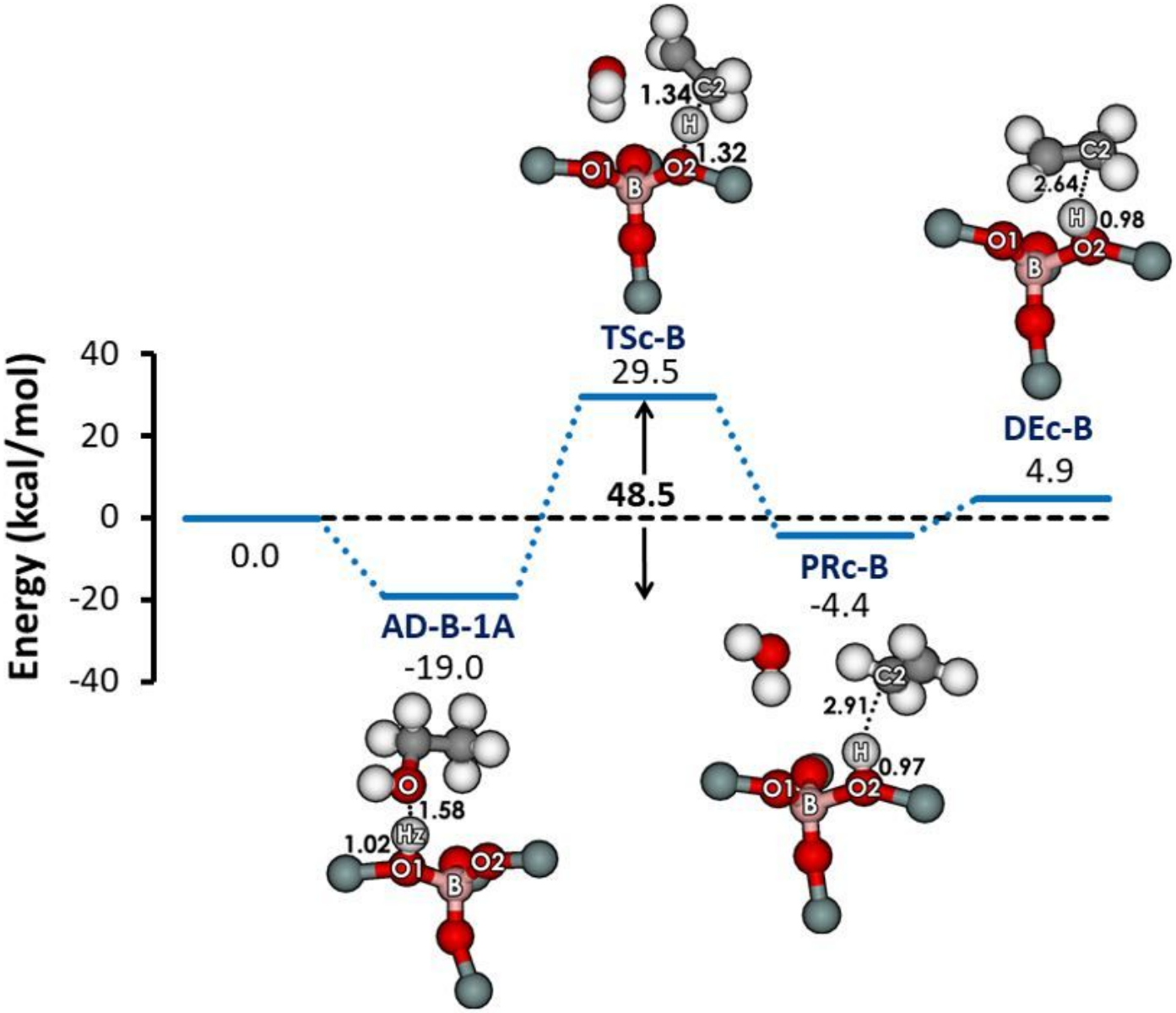

Figure 6

Energy profile for the concerted mechanism of ethanol to ethylene on 5T:34T model of H-[B]-ZSM-5 zeolites with the embedded ONIOM (MP2/6-311+G(2df,2p):M06-2X/6-311+G(2df,2p)) // ONIOM (MP2/6-31G(d,p):M06-2X/6-31G(d,p)). Distances are given in Å and energies in kcal/mol.

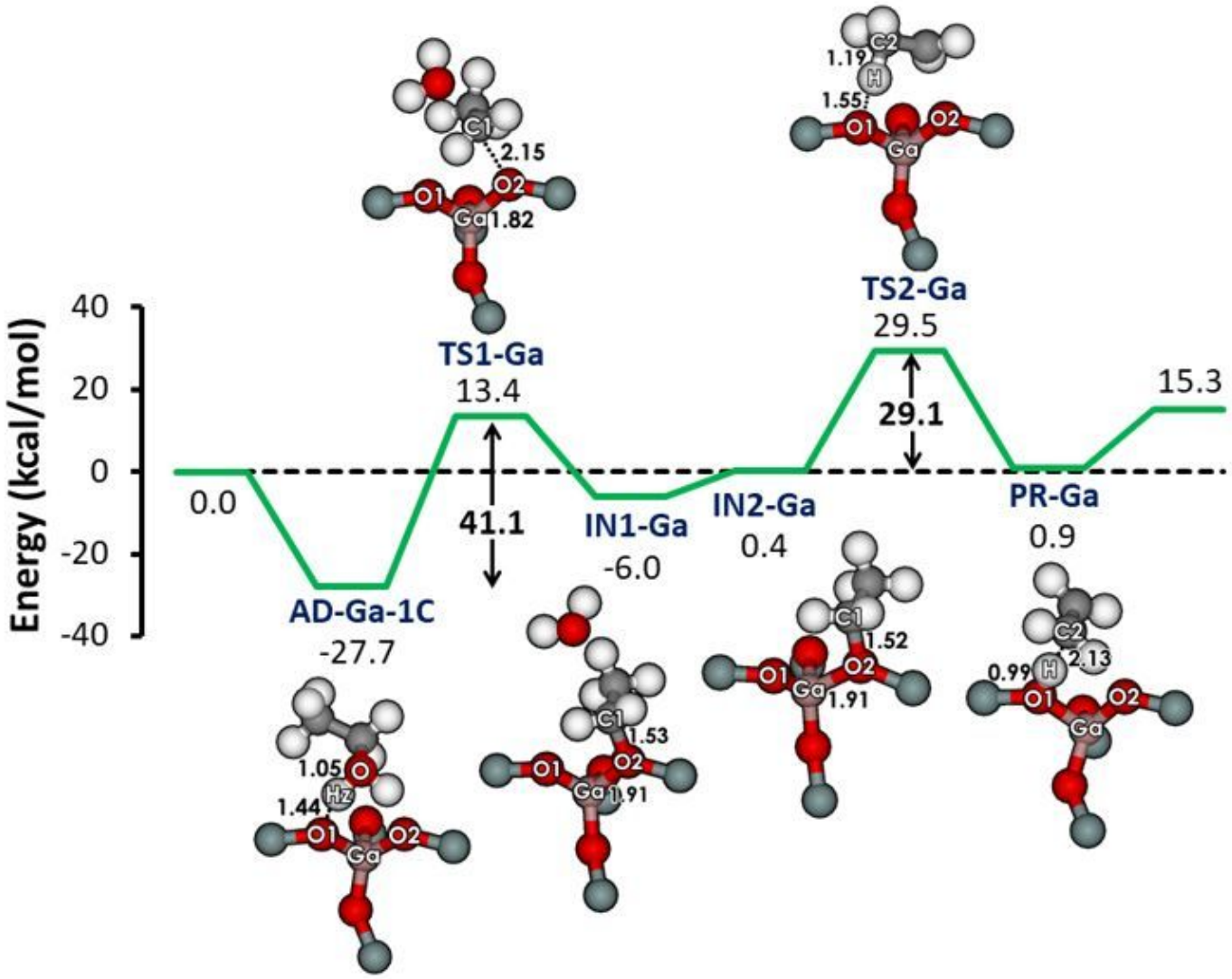

Figure 7

Energy profile for the stepwise mechanism of the dehydration reaction on the 5T:34T model of H-[Ga]-ZSM-5 zeolites calculated with the embedded ONIOM (MP2/6-311+G(2df,2p):M06-2X/6-311+G(2df,2p)) // ONIOM (MP2/6-31G(d,p):M06-2X/6-31G(d,p)). Distances are given in Å and energies in kcal/mol.

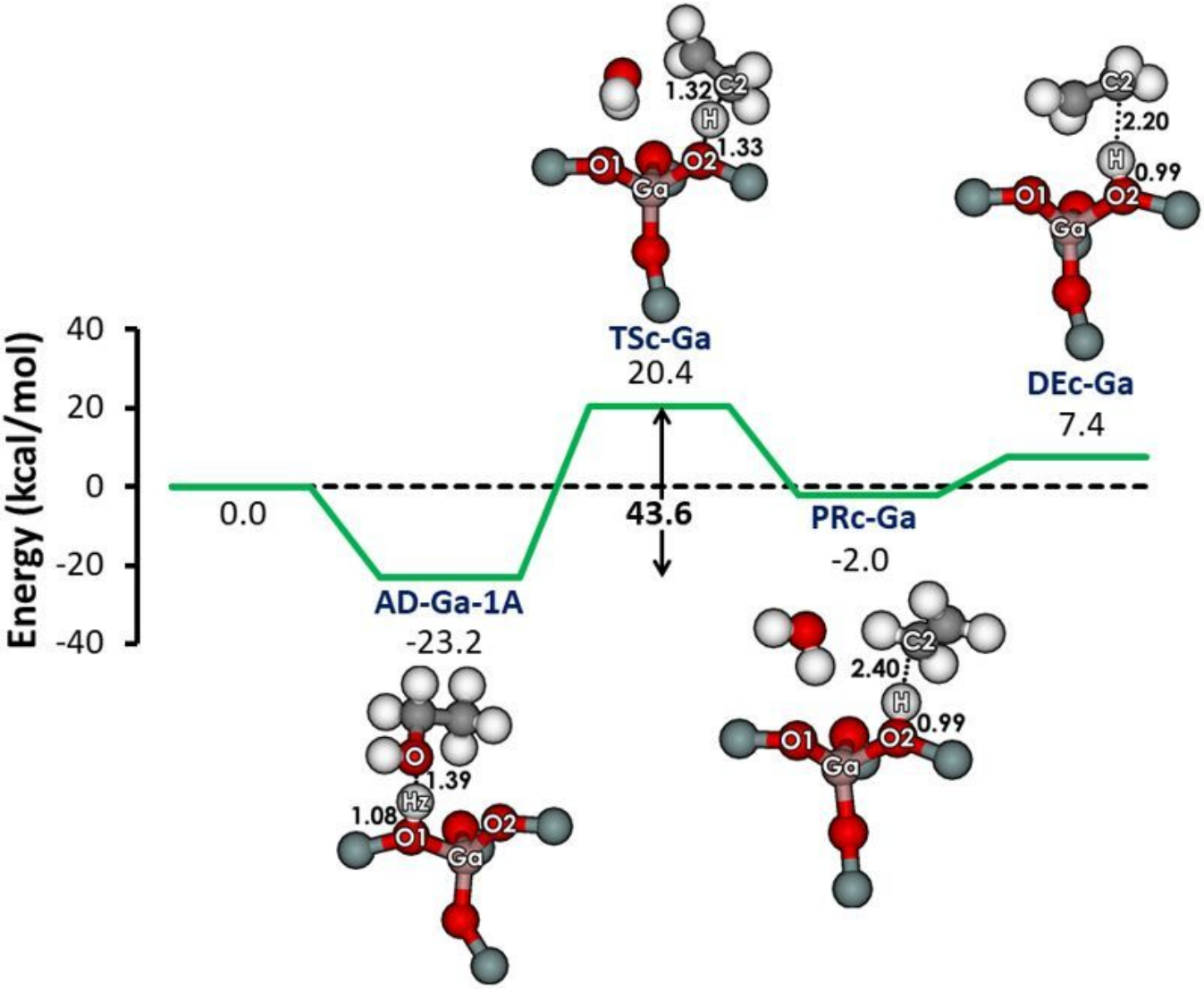

Figure 8

Energy profile for the concerted mechanism of the dehydration reaction on the 5T:34T model of H-[Ga]-ZSM-5 zeolites calculated with the embedded ONIOM (MP2/6-311+G(2df,2p):M06-2X/6-311+G(2df,2p)) // ONIOM (MP2/6-31G(d,p):M06-2X/6-31G(d,p)). Distances are given in Å and energies in kcal/mol.

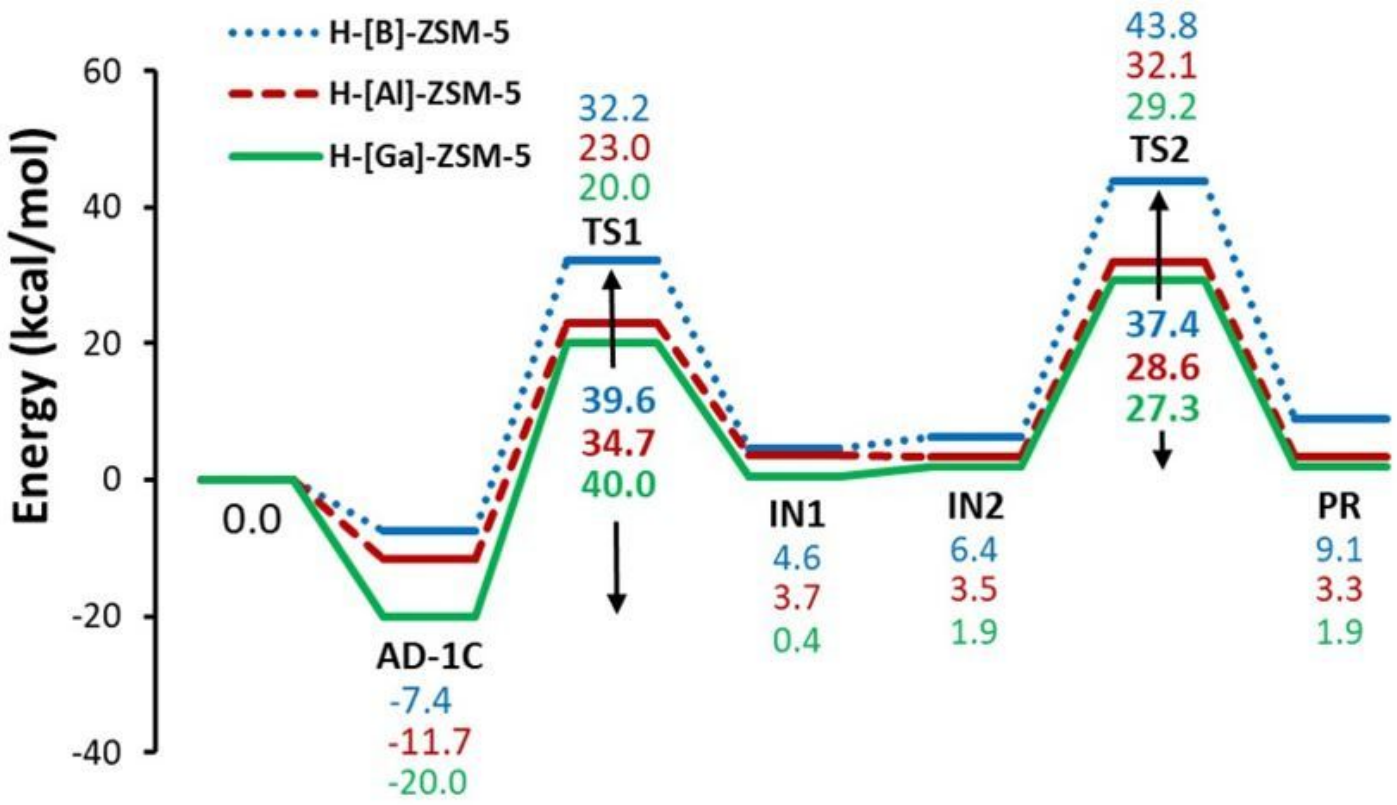

Figure 9

Energy profiles with the thermal free energies for the stepwise mechanism of on the three zeolites H-[B]-ZSM-5, H-[Al]-ZSM-5 and H-[Ga]-ZSM-5 zeolites as calculated with the ONIOM (MP2/6-31G(d,p):M06-2X/6-31G(d,p)) method.

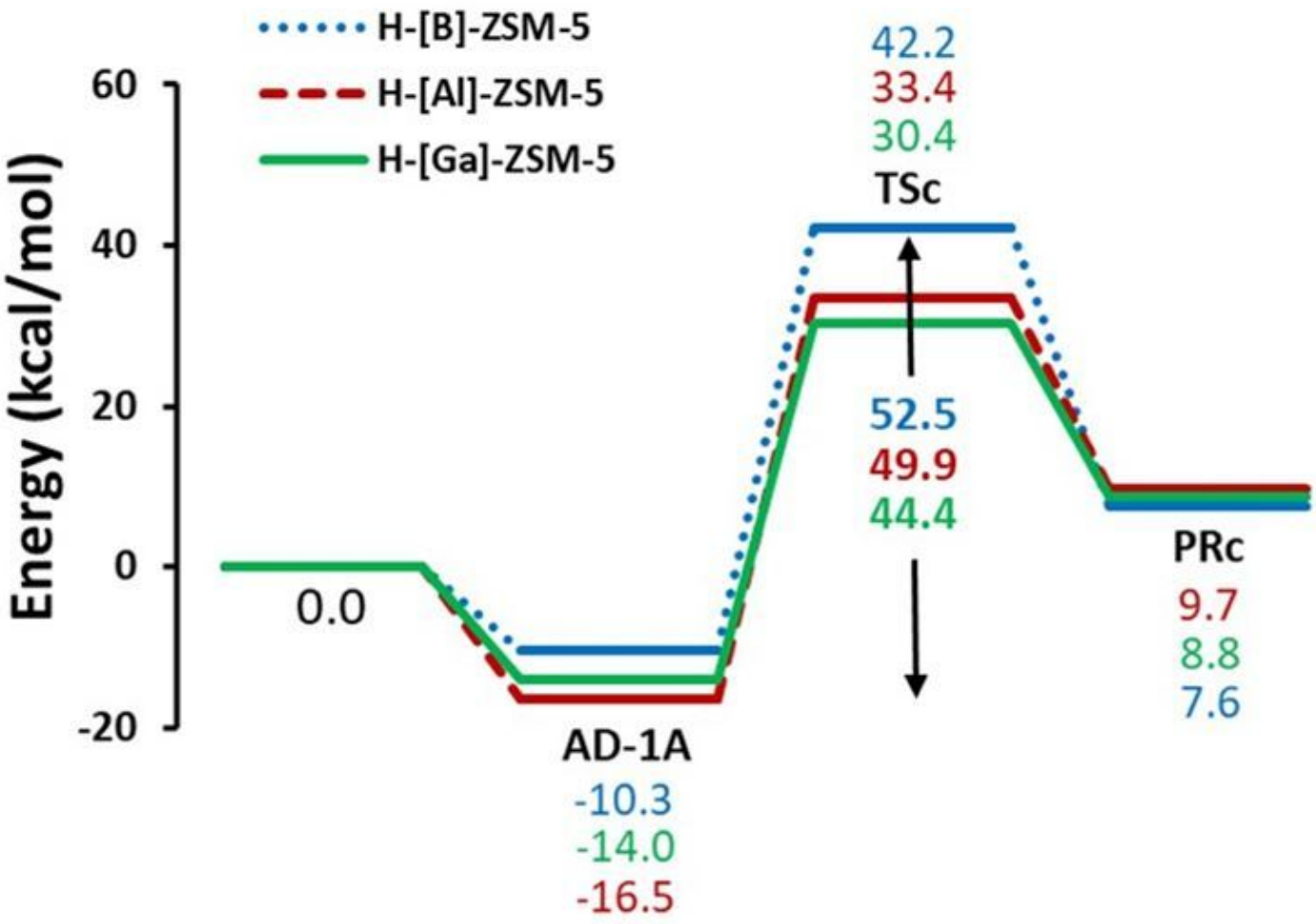

Figure 10

Energy profiles with the thermal free energies for the concerted mechanism of on the three zeolites H-[B]-ZSM-5, H-[Al]-ZSM-5 and H-[Ga]-ZSM-5 zeolites as calculated with the ONIOM (MP2/6-31G(d,p):M06-2X/6-31G(d,p)) method.

Supplementary Files

This is a list of supplementary files associated with this preprint. Click to download.

- scheme1.jpg
- 210517SupportinginformationZSM5.docx